Available online at www.sciencedirect.com
ScienceDirect
Journal of Hazardous Materials 159 (2008) 222–229
Journal of Hazardous Materials
www.elsevier.com/locate/jhazmat

Dependence of particle morphology and size on the mechanical sensitivity and thermal stability of octahydro-1,3,5,7-tetranitro-1,3,5,7-tetrazocine

Xiaolan Song, Yi Wang, Chongwei An, Xiaode Guo, Fengsheng Li *

National Special Superfine Powder Engineering Research Center, Nanjing University of Science & Technology, Nanjing 210094, China

Received 9 January 2008; received in revised form 1 February 2008; accepted 4 February 2008
Available online 13 February 2008

Abstract

Three kinds of octahydro-1,3,5,7-tetranitro-1,3,5,7-tetrazocine (HMX) samples with spherical (β-phase), needle (γ-phase) and polyhedral (β-phase) shapes were fabricated by wet milling, solvent/non-solvent and riddling methods, respectively. By changing the technical conditions, HMX powders with different particle sizes were obtained for each kind of sample. All as-prepared samples were characterized by laser granularity measurement, scanning electron microscopy (SEM) and X-ray diffractometry (XRD). Taking advantage of mechanical sensitivity tests, slow cook-off tests and differential scanning calorimetry (DSC) analysis, the mechanical sensitivity and thermal stability of HMX samples were found to depend on particle size and morphology. Results indicated that particle size played a significant role in the safety of HMX, and that morphology regulated the experimental results, i.e., for each kind of HMX samples, the mechanical sensitivity and thermal stability of HMX changed if the particle size differed. However, the trends of these changes exhibit much variance if the microstructure of the HMX particles is altered. Consequently, the difference in safety for these kinds of samples has to do with their specific morphology.

Keywords: HMX; Morphology; Particle size; Mechanical sensitivity; Thermal stability

1. Introduction

The wide application of octahydro-1,3,5,7-tetranitro-1,3,5,7-tetrazocine (HMX) has prompted vigorous efforts to understand and improve its safety. Among the factors affecting the safety of explosives (such as physical and chemical structures, charge diameter and density, etc.), microstructure and size of explosive particles play significant roles [1–4].

It is not strange to study the effects of particle size on mechanical sensitivity of explosives, but the reported results are controversial. Liu found that the friction sensitivity of explosives decreased almost linearly as the particle size was reduced from 154 to 10 μm [5]. However, Yang investigated the friction sensitivity of RDX particles sized 8.95, 12.78, 54.89 and 640 μm, and the results showed no self-consistent trend [6]. One report has even shown an inverse relationship between friction sensitivity and particle size of HMX [7]. Fortunately, the reports about impact sensitivity tests were more consistent, i.e., the impact sensitivity of explosive always fell as the particles size decreased. Zhang compared the impact sensitivity of HMX with different particle sizes and found that the explosive probability decreased significantly if the particles size is less than 2 μm, which is attributed to the slighter crystal deficiency inside the smaller explosive particles [8,9]. Simpson et al. also found that explosives with smaller particle size are more difficult to ignite, but that combustion following ignition has an increased likelihood of resulting in detonation [10,11].

The effect of morphology on the safety and stability of explosive particles is also important. However, few researchers addressed this factor, which may be the cause of the discrepancy noted above. For example, if we study the relationship between mechanical sensitivity and particle size, we should select HMX particles with similar microstructure. Otherwise, the results would fluctuate greatly because the potential factor, i.e., the effect of morphology is neglected. Herein, we used three methods to fabricate three kinds of HMX samples with differing

* Corresponding author. Tel.: +86 025 84315942.
E-mail address: songxiaolan00@126.com (F. Li).

0304-3894/$ – see front matter © 2008 Elsevier B.V. All rights reserved.
doi:10.1016/j.jhazmat.2008.02.009

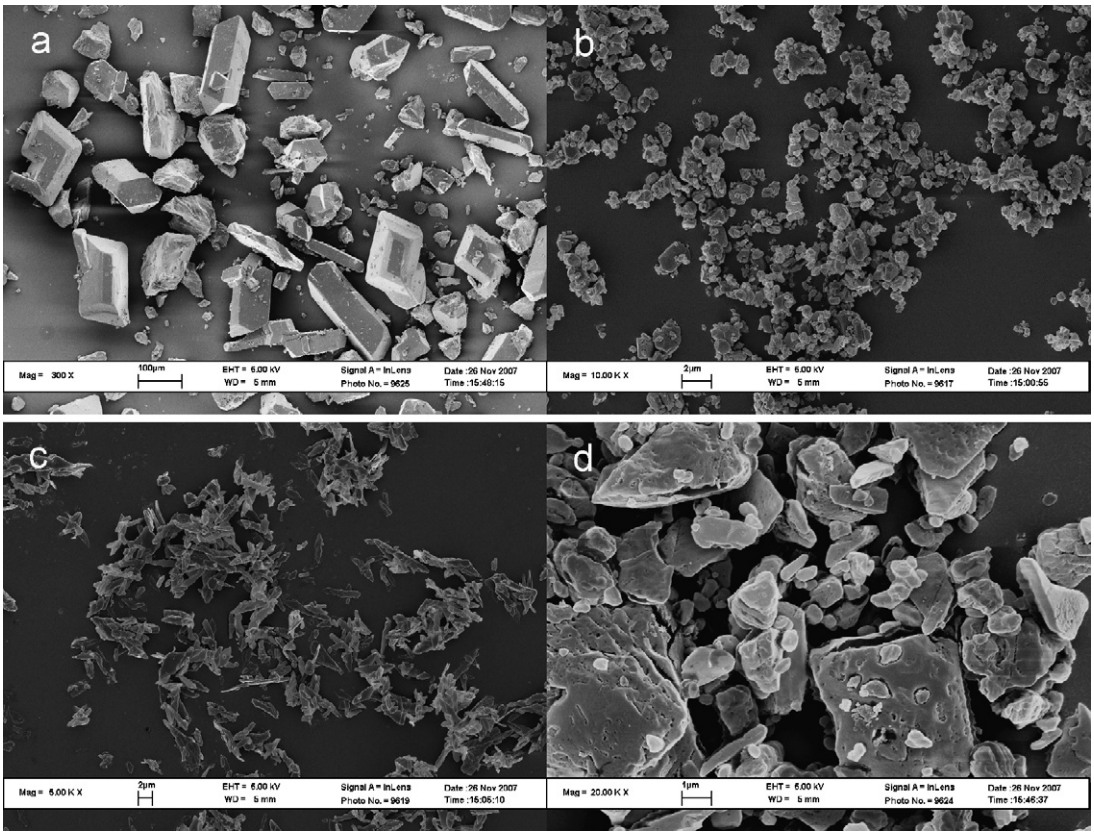

Fig. 1. SEM images of HMX samples: (a) raw HMX powders, $d_{50} = 85.9\ \mu m$; (b) prepared by milling, $d_{50} = 0.6\ \mu m$; (c) prepared by solvent/non-solvent method, $d_{50} = 2.98\ \mu m$; (d) prepared by riddling, $d_{50} = 3.26\ \mu m$.

morphologies. For each kind of HMX samples, the effect of particle size on their safety is studied. Furthermore, as a highlight of this study, the influence of microstructure of HMX particles on its safety is discussed in detail.

2. Experimental

2.1. Materials and fabrication

Raw HMX powders ($d_{50} = 85.9\ \mu m$, $d_{90} = 258.2\ \mu m$) were purchased from the Yinguang chemical plant of China. Using wet riddling, wet milling and solvent/non-solvent methods, three kinds of HMX samples were made from raw HMX. By controlling technical parameters, HMX particles with different average particle sizes (d_{50}) were obtained within each of the three kinds of samples (shown in Table 1).

2.2. Samples test

Sample morphologies were examined using a LEO field-emission scanning electron microscope (SEM). Particle size and size distribution of samples were measured using a Master Sizer Instrument. An HGZ-1 impact instrument was used to test the impact sensitivity of HMX samples. Each sample (35 mg) was tested 25 times to obtain a H_{50}. (The H_{50} value represents the height from which dropping a 5 kg weight will result in an explosive event in 50% of the trials.) With four replicate tests, an average value of H_{50} was calculated. A WM-1 friction instrument ($80 \pm 1^\circ$, 3.0 MPa) was employed to test the friction sensitivity of samples. Each sample (20 mg) was tested 25 times and an explosive probability P (%) was obtained. An average value of P was estimated with four replicate tests. In the slow cook-off test, the heating rate of each sample (3 g, charge Ø 10) was $3\ ^\circ C\ min^{-1}$. The self-accelerated heating of explosive charges was logged to estimate the thermal sensitivity of HMX samples. Differential scanning calorimetry (DSC) of samples was performed on a TA Model Q600 differential scanning calorimeter under a floating N_2 atmosphere ($10\ mL\ min^{-1}$). The heating rates for each sample were 5, 10 and $20\ ^\circ C\ min^{-1}$. Phase changes were detected using a Bruker Advance D8 X-ray diffractometer (XRD), using Cu Kα radiation at 40 kV and 30 mA.

3. Results

3.1. Sample characterization

Fig. 1 provides SEM images of raw HMX powders and part of as-prepared samples. The differences in morphology among the four kinds of samples shown above are obvious. The raw HMX (Fig. 1(a)) has prismatic type microstructure with smooth particle surfaces. SEM image of Fig. 1(b) shows that HMX particles prepared after several hours of wet milling yield the nearly spherical crystal morphology. In Fig. 1(c), groups of needle-

Table 1
Fabrication of samples with different morphology and particle size

Methods	Medium	Technical parameters	d_{50} (μm)
Wet riddling	Alcohol (95 wt.%)	Size of sieves	3.26, 21, 63, 82, 125 and 230
Wet milling	Alcohol (95 wt.%), ZrO_2 balls (0.8–2.5 mm)	Milling time, flow velocity of medium	0.6, 4.5, 10.9, 21 and 56
Solvent/non-solvent	Dimethyl sulfoxide (solvent), aqueous solution of emulsifier (non-solvent)	Stirring rate, temperature difference between solvent and non-solvent	2.98, 4.8, 10.2 and 16.1

Table 2
Analysis results of XRD in Fig. 2

Samples in Fig. 2	Morphology	d_{50} (μm)	Phases	X_s (nm)
a	Prism	85.9	β	62.5
b	Spherical	0.6	β	43.4
c	Polyhedron	3.26	β	28.6
d	Needle	2.98	γ	19.3

shaped particles representing loose agglomerates are visible, whereas the HMX particles prepared by wet riddling present some unregulated polyhedral microstructure with very coarse surfaces in Fig. 1(d).

Samples imaged in Fig. 1 were selected, and their phases were analyzed by X-ray diffractometry. MID jade5.0 software was employed to fit their diffractive peaks and calculate the average crystallite size (X_s) of samples. XRD patterns and analysis results are shown in Fig. 2 and listed in Table 2, respectively.

In Fig. 2, the XRD patterns of HMX samples shows clearly that the raw HMX and the samples prepared by wet riddling and milling exist as the same crystal phase—beta (β). Relating to their fabricated methods in point, this result is not surprising. However, unlike the patterns of a–c, the crystallinity of HMX sample prepared by solvent/non-solvent method is verified in Fig. 2(d), which displays the pattern of d as γ-HMX. It is evident that adoption of different prepared methods not only can change the surface morphology of HMX particles but also may transform their crystal phase.

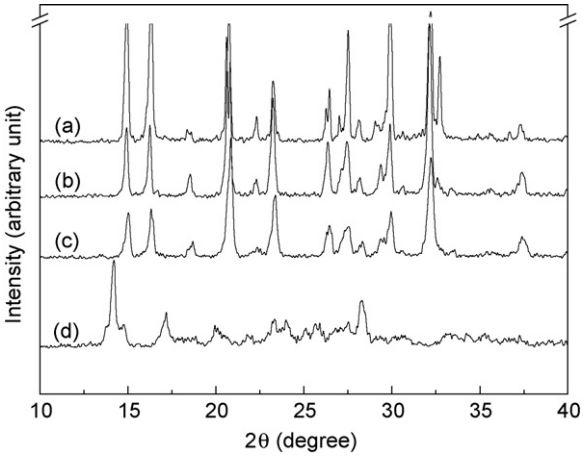

Fig. 2. XRD patterns of HMX samples: (a) raw HMX powders, d_{50} = 85.9 μm; (b) by milling, d_{50} = 0.6 μm; (c) by riddling, d_{50} = 3.26 μm; (d) by solvent/non-solvent method, d_{50} = 2.98 μm.

3.2. Mechanical sensitivity analyses

Small-scale mechanical sensitivity tests were performed on all HMX samples prepared in this report, and the results of these tests are shown in Fig. 3. Each plot in Fig. 3 shows two curves corresponding to changes in impact and friction sensitivity as a function of particle size. For spherical β-HMX samples, the H_{50} increases as the particle size decreases—especially within the scale of 0.6–21 μm. The trend indicates that small, spherical β-HMX particles are less sensitive to impact force. In the friction test, however, the result reverses and the friction sensitivity increases gradually as particle size decreases. For needle-like γ-HMX samples, the impact and friction sensitivities both linearly increase with increasing particle size from 2.98 to 16.1 μm. For polyhedral β-HMX samples, the plots of impact and friction sensitivity versus particle size show no obvious trend, i.e., the testing data do not increase or decrease regularly as a function of particle size.

On the other hand, the average value of H_{50} for needle-like γ-HMX samples ($\bar{H}_{50} = 17.1$ cm) is much lower than that for spherical ($\bar{H}_{50} = 54.1$ cm) and polyhedral ($\bar{H}_{50} = 45.5$ cm) samples. This implies that needle-like γ-HMX particles are quite sensitive to impact stimuli. Meanwhile, the average value of explosive probability ($\bar{P}$) of polyhedron β-HMX samples equals 32%, which is lower than that of spherical ($\bar{P} = 80\%$) and needle ($\bar{P} = 82\%$) samples.

3.3. Thermal stability analyses

3.3.1. Thermal sensitivity tests

Fig. 4 reveals the thermal sensitivity of three kinds of HMX samples as a function of particle size. It shows the influences of particle size and morphology on the self-accelerated heating of HMX. Plots a and b illustrate that the $\overline{T}_{break}$ of spherical and polyhedron β-HMX samples both tend to decrease as the particle size become larger, which implies that the smaller particles have higher thermal stability. While needle γ-HMX samples take itself on the opposite side, i.e., the smaller particles are easier to explode in the course of heating.

Compared to the experimental results for the three kinds of HMX samples, we find that the effect of morphology on the thermal sensitivity of HMX is obscure in that very little difference in average $\overline{T}_{break}$ values is seen for the different particle sizes. The average ($\overline{T}_{break}$) values of 273.0, 268.7, and 265.5 °C were measured for spherical, polyhedral and needle-like samples, respectively.

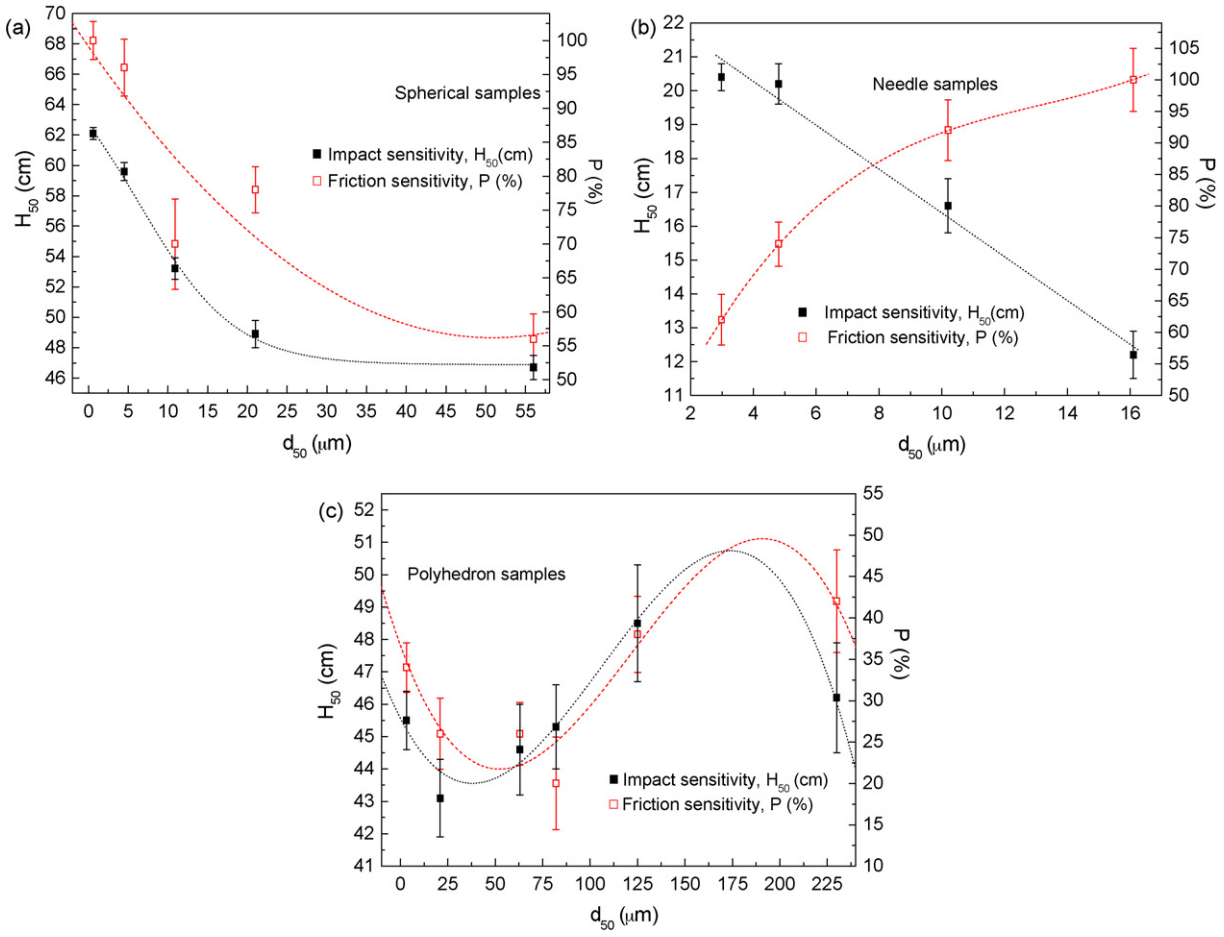

Fig. 3. Impact and friction sensitivities of HMX samples as a function of particle size: (a) by milling; (b) by solvent/non-solvent; (c) by riddling. The error bars represent one standard deviation of the average value obtained from four peering tests.

3.3.2. *Thermal decomposition tests*

Fig. 5 shows the DSC curves for HMX samples with different morphologies. These curves were acquired in N_2 atmosphere at heating rates of 5, 10 and 20 °C min^{-1}. In each case, the temperature of the exothermic peak and the decomposition heat (determined by the area of the primary peak in DSC curve) decrease with decreasing heating rate. However, the results for the different kinds of samples do not generally shift to the same extent at any given heating rate.

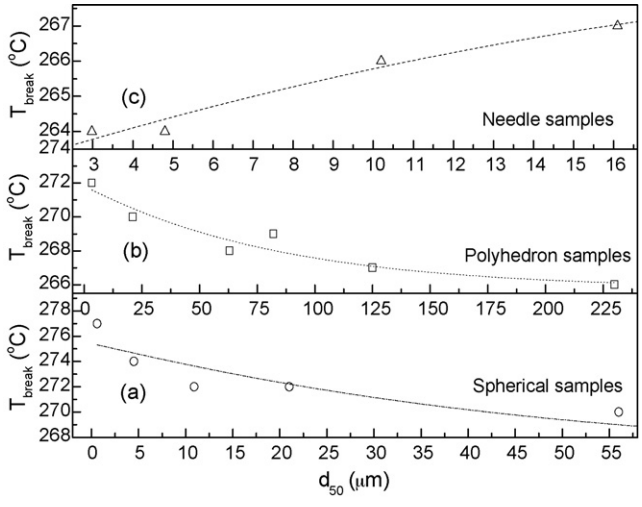

Fig. 4. Self-accelerated heating of HMX samples as a function of particle size: (a) by milling; (b) by riddling; (c) by solvent/non-solvent.

The Starink method is used in the kinetic evaluation when studying the effects of particle size and microstructure on apparent activation energies for thermal decomposition of HMX. It is an order of magnitude more accurate than others and follows the following equation [12,13]:

$$\ln\left(\frac{T_p{}^s}{\phi}\right) = A\frac{E_a}{RT_p} + C \tag{1}$$

where T_p is the temperature of exothermic peak in DSC curve, K; Φ is the heating rate, K min^{-1}; E_a is the activation energy, J mol^{-1}; s is a constant, and A is a constant which depends of the choice of s. In the case of the Kissinger method $s = 2$ and $A = 1$, the Ozawa method uses $s = 0$ and $A = 1.0518$, and the Starink method uses $s = 1.8$ and $A = 1.0070–1.2 \times 10^{-8}\,E_a$. The last method is employed to determine E_a of samples. Because the values of R^2 for the insets in Fig. 5 exhibit some difference with each other, the final apparent activation energy of each sample is expressed as an average value of E_a calculated from Starink's

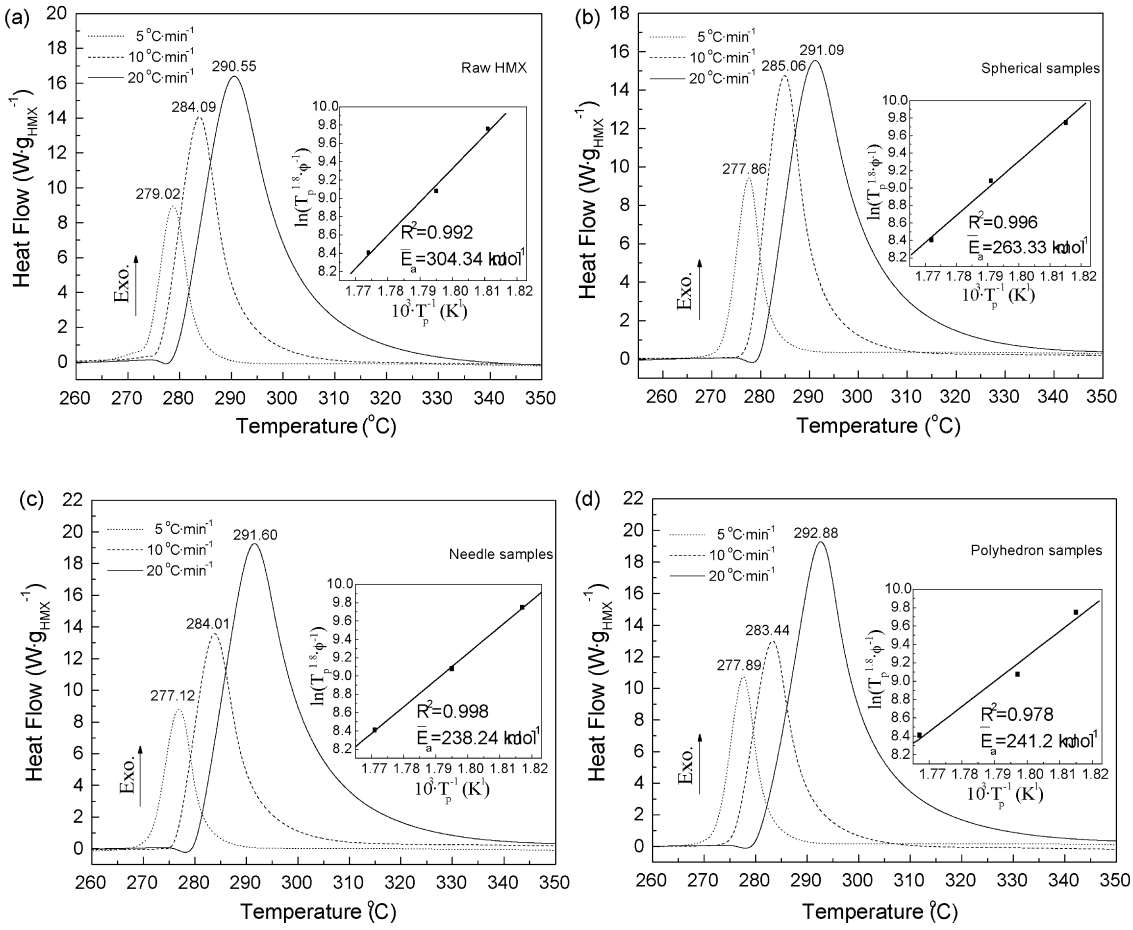

Fig. 5. DSC traces for HMX samples: (a) raw HMX powders, $d_{50} = 85.9\ \mu m$; (b) by milling, $d_{50} = 0.6\ \mu m$; (c) by solvent/non-solvent method, $d_{50} = 2.98\ \mu m$; (d) by riddling, $d_{50} = 3.26\ \mu m$. Each inset is a Starink' plot for the thermal decomposition peak of the DSC curves. Symbol R^2 is used to identify the linear coefficient of $\ln(T_p^{1.8}\Phi^{-1})$ to $1000 \times T_p^{-1}$.

formula with DSC data collected at every two heating rates

$$\bar{E}_a = \frac{E_{a(5-10\,K\,min^{-1})} + E_{a(5-20\,K\,min^{-1})} + E_{a(10-20\,K\,min^{-1})}}{3} \quad (2)$$

where $\bar{E}_a$ is the final apparent activation energy of thermal decomposition for a sample, $E_{a(5-10\,K\,min^{-1})}$, $E_{a(5-20\,K\,min^{-1})}$ and $E_{a(10-20\,K\,min^{-1})}$ are the activation energies calculated from expression (1) by Starink's method.

Fig. 6 shows the plots of $\bar{E}_a$ versus particle size for the three HMX morphologies. In Fig. 6, for each kind of samples, the change of $\bar{E}_a$ does not appear to change significantly with particle size. However, comparing different sample morphologies, the average value (calculated using the data at different d_{50}) of $\bar{E}_a$ for spherical particles ($\bar{\bar{E}}_a = 263.45\ kJ\ mol^{-1}$) is higher than that for polyhedral ($\bar{\bar{E}}_a = 243.7\ kJ\ mol^{-1}$) and needle-like ($\bar{\bar{E}}_a = 239.19\ kJ\ mol^{-1}$) particles. This result implies that the needles decompose easily, and that the thermal stability of the spherical β-HMX particles takes on optimal above all, which are similar to the experimental results in Fig. 4.

Noticeably, in Fig. 6, the point for raw β-HMX is quite isolated from the values for polyhedral samples. Ostensibly, the raw β-HMX should yield results similar to the sieved samples, since they are kin. Essentially, a large difference exists between their particle size distributions.

Fig. 7 displays particle size distribution diagrams of raw β-HMX powders and β-HMX samples prepared by riddling. The size distribution of raw particles in Fig. 7(a), spanning from 0.1 nm to 1000 μm, is quite broad. While the sieved samples differ, each diagram presents a regular, narrow and dominant curve in Fig. 7(b–d). In our previous studies for RDX, we found that although two kinds of RDX powders have almost the same d_{50}, the activation energy of the sample with broad size distribution (0.1–90 μm, $d_{50} = 5.6\ \mu m$, $E_a = 135\ kJ\ mol^{-1}$) is higher than that of a sample with narrow size distribution (0.3–15 μm, $d_{50} = 4.9\ \mu m$, $E_a = 119\ kJ\ mol^{-1}$). Therefore, we conclude that the over-broad size distribution of raw β-HMX results in the highest activation energy, which is exhibited in Fig. 6.

4. Discussion

In combining the experimental results and theories together, we suppose that the unique microstructure of each kind of HMX particles relates to the "hot spot" growth mechanism [14]. In fric-

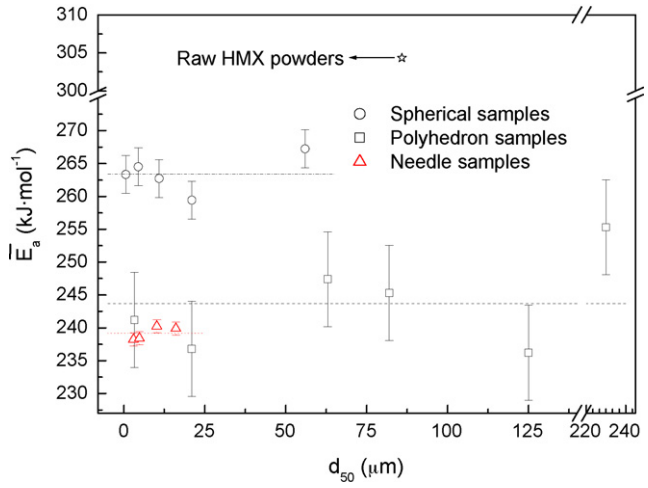

Fig. 6. $\overline{E}_a$ for HMX vs. particle size. The error bars represent the standard deviation for the average value of $\overline{E}_a$.

tion sensitivity tests, the friction among HMX particles is the main factor forming "hot spots", which then cause detonation. For spherical β-HMX samples, the contact area upon particles surfaces and bulk density are apparently higher than those of needle particles when they undergo the same frictional action. Therefore, under the same condition, the spherical powders may produce more heat (especially the smaller particles), which will increase the likelihood of forming a "hot spot". In fact, the nee-

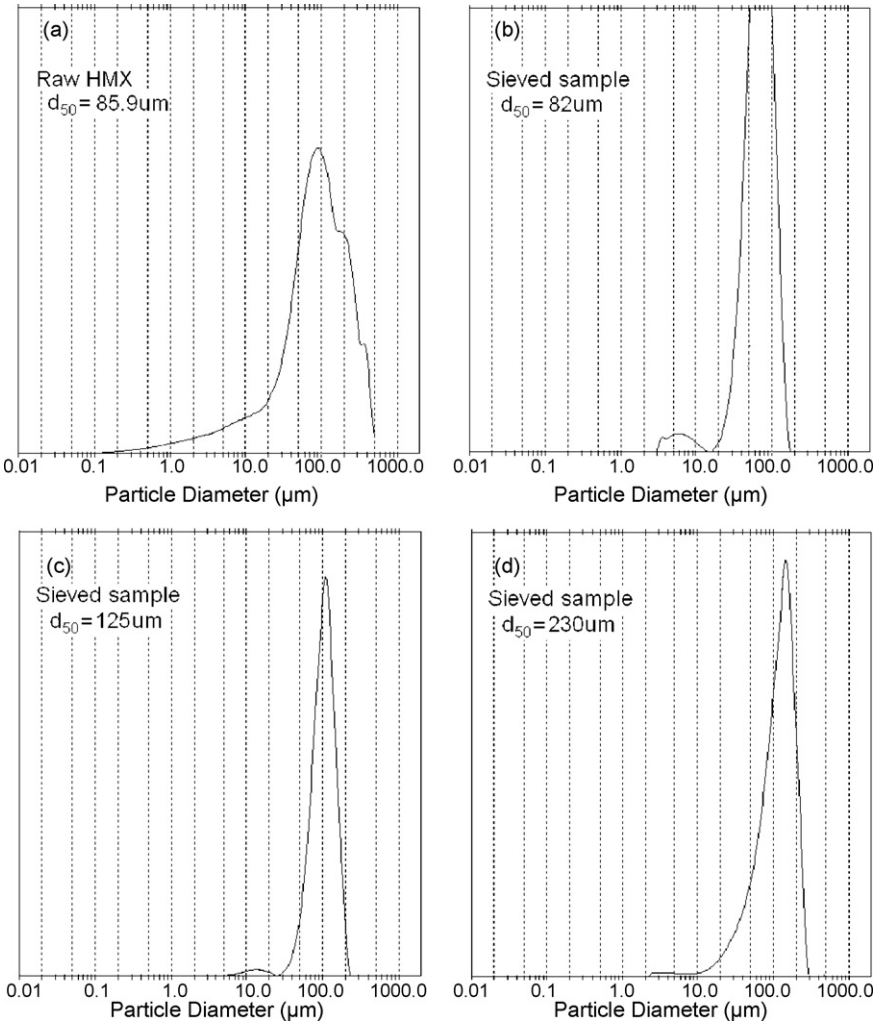

Fig. 7. Size distribution diagrams of HMX samples.

dle γ-HMX particles of larger size also present higher friction sensitivity. It may owe to the much crystal deficiencies inside their particles. Therefore, larger needle particles can be crushed, breaking into fragments due to external force (by contrast, the larger spherical β-HMX particles are not easy fragmented in this way). Those spiculate fragments chafe against one another, causing high heat release and explosion.

In the impact sensitivity tests, the friction among explosive particles becomes a subordinate factor, and the influence of crystal deficiencies inside HMX particles dominates. When explosive particles undergo exoteric impact action, "hot spots" grow preferentially with the weak interface of crystals via intervening, spalling, rolling and smashing. This mechanism is appropriate when explaining why needle-like samples exhibit higher impact sensitivity because of their high crystallite asymmetry. However, spherical β-HMX particles not only have uniform texture and few crystal deficiencies, but also contact tightly by means of their smooth and curved surfaces. Furthermore, there are plenty of tiny air holes among the spherical particles, which can cushion a blow from the impact action. Accordingly, spherical β-HMX samples present the lowest impact sensitivity.

In terms of thermal stabilities, the thermal conductivity of the explosive plays a significant role. In general, as the particle size of the explosive decreases, the specific surface area and the amount of atoms located at the particle surface increase, which mean that the outer electronic orbital extends and the atoms' vibrating space expands. These changes result in an improvement in thermal conductivity among explosive particles [11,15,16]. As a result of higher thermal conductivity, the heat released by thermal decomposition can be dissipated in time to prevent explosive decomposition, and further decomposition is limited. Accordingly, smaller particles should present higher thermal stabilities. However, in our experiments, needle-shaped γ-HMX particles are an exception, i.e., the smaller needle particles are easier to explode in the cook-off test and exhibit lower activation energy in thermal analysis. This phenomenon is mostly attributed to their unique morphology. In fact, for needle-shaped particles, the average particle size (d_{50}) measured by laser granularity measurement cannot represent their actual dimensions. Abstractly, for a needle-shaped particle, the size at the "top-end" may be of submicron and even nanometer scales although the d_{50} of whole powders equal to 2.98 μm. Meanwhile, as the d_{50} of needle particles decreases, the tiny "top-end" would be more and smaller, which present high reactivity and decompose firstly with a mass of heats releasing in heating procedure. If the heat generated is greater than the heat which is radiated, the temperature of the explosive system climbs continuously, which further accelerates thermal decomposition of the explosive. Perhaps due to such a self-catalytic reaction, the needle-like samples exhibit the lowest values of $\bar{T}_{\text{break}}$ and $\bar{\bar{E}}_{\text{a}}$.

Another factor affecting explosive safety is the different crystal phases among the three kinds of samples. In general, HMX can exist as α, β, γ or δ four phases, and β-HMX has the highest stability [17]. With a 5 kg hammer, Ye elicited a H_{50} of 33 cm for β-HMX (d_{50} = 125–500 μm), which is much larger than the H_{50} (7 cm) of γ-HMX (d_{50} = 10 μm) [17]. This result is consistent with our tests. In addition, the thermal stabilities of HMX samples are related to their X_{s} (listed in Table 2), i.e., explosive particles with smaller crystallite may decompose first in the course of heating.

5. Conclusion

In Section 1, we not only summarized many reports about the effect of particle size on the mechanical sensitivity of explosives, but also showed the discrepancies among them. Therein, we speculated that the different microstructures of explosive particles caused the inconsistency in previous studies' experimental results. In order to confirm our supposition, i.e., to investigate the influence of morphology on mechanical sensitivities and thermal stabilities of explosive, three kinds of HMX samples with spherical, needle-like and polyhedral microstructures have been fabricated by wet milling, solvent/non-solvent and wet riddling methods, respectively. Meanwhile, via controlling the size of sieves, milling time and temperature difference between solvent and non-solvent, etc., HMX with different particle size were obtained within each kind of samples. The results of our tests expectably indicate that the safety of HMX is affected by particle size, but also depends strongly on the microstructure of HMX particles. As a result, it is possible to obtain two results under the same experimental conditions if two samples have similar dimension and different morphologies. For spherical β-HMX samples, the smaller particles have higher friction sensitivity. However, for the needle-shaped γ-HMX particles, the explosive probability P (%) falls along with decreasing particle size.

Furthermore, on the whole, the spherical β-HMX samples have lower impact sensitivity, higher friction sensitivity and higher thermal stability. The needle-shaped γ-HMX samples have higher impact sensitivity, lower friction sensitivity and lower thermal stability. The mechanical sensitivity and thermal stability of polyhedral samples are more moderate and the data display no obvious trends as a function of particle size except that in slow cook-off tests, their self-accelerated temperature gently increases as the particle size decreases.

Acknowledgements

This work was performed by several research groups in our center. The authors would like to thank Chengfang Che of National Special Superfine Powders Engineering Research Center in Nanjing University of Science & Technology for her enthusiastic support in granularity measurements and DSC analysis, and Dr. Haridwar Singh of High Energetic Materials Research Lab (HEMRL) of India who provided many helpful suggestions for our experiments.

References

[1] C.R. Siviour, M.J. Gifford, S.M. Walley, Particle size effects on the mechanical properties of a polymer bonded explosive, J. Mater. Sci. 39 (2004) 1255–1258.

[2] J.R. Luman, B. Wehrman, K.K. Kuo, Development and characterization of high performance solid propellants containing nano-sized energetic ingredients, Proc. Comb. Inst. 31 (2007) 2089–2096.

[3] J.H. ter Horst, R.M. Geertman, G.M. van Rosmalen, The effect of solvent on crystal morphology, J. Crystal Growth 230 (2001) 277–284.
[4] Pelin Karakaya, Mohammed Sidhoum, Christos Christodoulatos, Aqueous solubility and alkaline hydrolysis of the novel high explosive hexanitrohexaazaisowurtzitane (CL-20), J. Hazard. Mater. B120 (2005) 183–191.
[5] Y.C. Liu, J.H. Wang, C.W. An, Effect of particle size of RDX on mechanical sensitivity, Chinese J. Expl. Prop. 27 (2004) 7–9.
[6] B.L. Yang, R.Y. Chen, X.H. Cao, Influence of particle size of RDX on the detonation properties, Chinese Initiators Pyrotech. 3 (2004) 50–56.
[7] T.S. Chen, Y.R. Zhang, Y.H. Zhang, Study on the influence of particle size on the mechanical sensitivity of HMX, Chinese Sichuan Ordn. J. 5 (2006) 27–28.
[8] X.N. Zhang, G.G. Xu, J.P. Xu, A study about impact sensitivity of ultrafine HMX and RDX, Chinese J. Expl. Prop. 1 (1999) 33–36.
[9] C.L. Lv, J.L. Zhang, Influence of particle size on the impact sensitivity of HMX, Chinese Expl. Shock Waves 23 (2003) 472–474.
[10] R.L. Simpson, P.A. Urtiew, D.L. Omellas, CL-20 performance exceeds that of HMX and its sensitivity is moderate, Prop. Expl. Pyro. 22 (1997) 249–255.
[11] Shuji Ye, Kenichi Tonokura, Mitsuo Koshi, Energy transfer rates and impact sensitivities of crystalline explosives, Comb. Flame 132 (2003) 240–246.
[12] R.H. Fan, H.L. Lu, K.N. Sun, Kinetics of thermite reaction in Al–Fe_2O_3 system, Thermochim. Acta 440 (2006) 129–131.
[13] S. Vyazovkin, C.A. Wight, Kinetics in solids, Annu. Rev. Phys. Chem. 48 (1997) 125–149.
[14] R.W. Armstrong, H.L. Ammon, W.L. Elban, Investigation of hot spot characteristics in energetic crystals, Thermochim. Acta 384 (2002) 303–313.
[15] X.J. Feng, X.F. Wang, Z.L. Han, The study of charging size influence on the response of explosives in slow cook-off test, Chinese Expl. Shock Waves 25 (2005) 285–288.
[16] T.M. Tillotson, A.E. Gash, R.L. Simpson, Nanostructured energetic materials using sol–gel methodologies, J. Non-Cryst. Solids 285 (2001) 338–345.
[17] Y.Y. Peng, X.M. Cao, L. Ye, Theory and Application of Crystallography for Explosives, 1, Armamentarii Press, Beijing, 1995.